Pentamethylcyclopentadienyl Ruthenium "Pogo Stick" Complexes with Nitrogen Donor Ligands

SUPPORTING INFORMATION

Table of Contents

S1 Single crystal X-ray diffraction

Crystals were mounted on glass fibres (**1**, **2**, **3** and **5**) or on top of a human hair (both polymorphs of **4**) in per-fluorinated inert oil. Data were recorded on an Oxford Diffraction Nova A diffractometer using mirror-focused Cu K_α radiation. Absorption corrections were based on multi-scans and for compound **1** and the monoclinic polymorph of **4** additional absorption correction based on face indexing and integration on a Gaussian grid was applied. Data reduction was performed with CrysalisPro.[1] The structures were solved by intrinsic phasing with SHELXT-2014/5[2] (**1** and the monoclinic polymorph of **4**) or SHELXS-97[3] (**2**, **3**, the triclinic polymorph of **4** and **5**) and refined on F^2 using the program SHELXL-2018/3 [4]. H atoms in all the reported crystal structures were placed in idealized positions and refined using a riding model. Exceptions are noted in the following special features section.

Complete data have been deposited at the Cambridge Crystallographic Data Centre under the numbers 1870526 - 1870531.

These data can be obtained free of charge from www.ccdc.cam.ac.uk/data_request/cif.

Special Features

Compound **1**: The C_5Me_5 as well as the allyl ligand were refined with a discrete disorder model. SADI restraints were applied to the C_5Me_5 moiety which was showing an occupation of 51 % for the major component. The major component of the allyl moiety was occupied by 85 %.

Compound **3**: The hydridic hydrogens atoms were refined freely with a SADI restraint on the ruthenium hydrogen distances.

Compound **4** (triclinic): One isopropyl group is disordered and was refined on two positions (SADI and ISOR restraints were applied).

Table S1. Crystal structure data

Compound	**1**	**2**	**3**
CCDC	1870529	1870526	1870528
Formula	$C_{19}H_{36}RuSi_2$	$C_{16}H_{33}NRuSi_2$	$C_{26}H_{47}NRu_2Si_2$
M_r	421.73	396.68	631.96
Habit	Red plate	dark-red, cut plate	black, irregular
Cryst. size (mm)	0.19 x 0.14 x 0.03	0.18 x 0.18 x 0.05	0.20 x 0.20 x 0.05
Crystal system	monoclinic	triclinic	orthorombic
Space group	$P2_1/c$	$P\bar{1}$	*Pbca*
Temperature (°C)	–173	–173	–143
Cell constants:			
a (Å)	11.6739(4)	8.6495(3)	14.7656(4)
b (Å)	11.5368(4)	9.6051(4)	24.5786(7)
c (Å)	16.0349(4)	13.2177(5)	31.6576(7)
α (°)	90	108.900(4)	90
β (°)	93.000(4)	96.188(3)	90
γ (°)	90	104.291(4)	90
V (Å^3)	2156.61(12)	985.42(7)	11489.1(5)

Z	4	2	16
D_x (Mg m^{-3})	1.299	1.337	1.461
μ (mm^{-1})	6.894	7.524	9.398
F(000)	888	416	5216
λ (Å)	1.54184	1.54184	1.54184
$2\Theta_{max}$	136.49	152.22	152.60
Refl. measured	19491	40300	133678
Refl. indep.	3936	4095	12009
R_{int}	0.0653	0.0430	0.0762
Parameters	320	203	597
Restraints	70	0	6
$wR2(F^2$, all refl.)	0.0834	0.0583	0.0686
$R1(F$, >4σ(F))	0.0332	0.0229	0.0282
S	1.035	1.069	1.040
max.Δρ (e Å^{-3})	0.634 / -0.637	0.313 / -1.062	0.782 / -0.990

Compound	**4**	**4**	**5**
CCDC	1870527	1870530	1870531
Formula	$C_{37}H_{51}N_3Ru$	$C_{37}H_{51}N_3Ru$	$C_{42}H_{60}N_4ORu$
M_r	638.87	638.87	738.01
Habit	black, irregular	black, irregular	dark-red, cut plate
Cryst. size (mm)	0.20 x 0.16 x 0.12	0.21 x 0.17 x 0.13	0.20 x 0.12 x 0.04
Crystal system	triclinic	monoclinic	monoclinic
Space group	$P\bar{1}$	$P2_1/n$	$P2_1/c$
Temperature (°C)	–143	–173	–173
Cell constants:			
a (Å)	10.3355(4)	10.461444(8)	10.4313(3)
b (Å)	10.4767(4)	18.55835(12)	18.5572(4)
c (Å)	19.0232(7)	18.31024(14)	20.5081(4)
α (°)	83.065(3)	90	90
β (°)	79.713(3)	98.1772(8)	95.352(2)°
γ (°)	60.953(4)	90	90
V (Å^3)	1770.44(13)	3518.74(4)	3952.57(16)
Z	2	4	4
D_x (Mg m^{-3})	1.198	1.206	1.240
μ (mm^{-1})	3.771	3.794	3.472
F(000)	676	1352	1568
λ (Å)	1.54184	1.54184	1.54184
$2\Theta_{max}$	152.52	152.47	152.32
Refl. measured	73296	177373	160975
Refl. indep.	7365	7341	8253
R_{int}	0.0533	0.0614	0.1042
Parameters	413	383	449
Restraints	51	0	0
$wR2(F^2$, all refl.)	0.0681	0.0909	0.0338
$R1(F$, >4σ(F))	0.0270	0.0329	0.0849
S	1.055	1.030	1.051
max.Δρ (e Å^{-3})	0.260 / -0.826	1.044/ -0.440	0.509 / -0.866

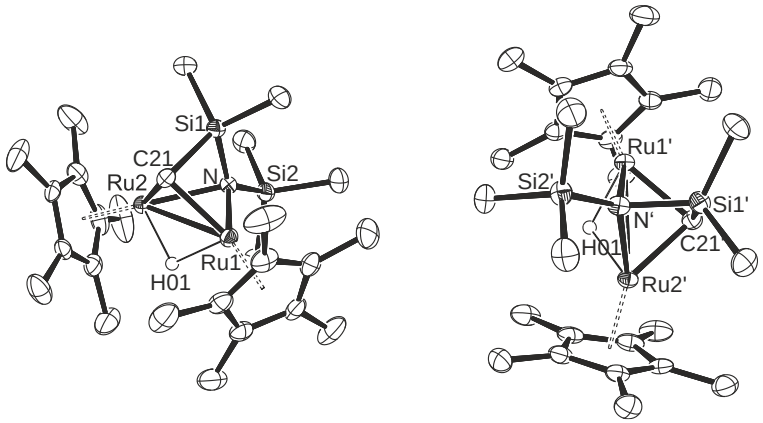

Figure S1. Molecular structure of compound **3** with thermal displacement parameters drawn at 50% probability. Hydrogen atoms except of H01 and H01‘ are omitted for clarity. Selected bond lengths [Å] and angles [°]: Ru1–Ru2 2.7066(3), Ru1–N 2.142(2), Ru2–N 2.152(2), Ru1–C21 2.037(3), Ru2–C21 2.014(3), Si1–C21 1.902(3), Si1–N 1.743(2), Si2–N 1.723(2), Si1–C21–Ru1 85.94(11), Si1–C21–Ru2 86.92(11), Ru2–C21–Ru1 83.83(10), Ru2–N–Ru1 78.15(8); Ru1‘–Ru2‘ 2.7065(3), Ru1‘–N1‘ 2.170(2), Ru2‘–N‘ 2.143(2), Ru1‘–C21‘ 2.013(3), Ru2‘–C21‘ 2.031(3), Si1‘–C21‘ 1.901(3), Si1‘–N‘ 1.750(2), Si2‘–N‘ 1.721(2), Si1‘–C21‘–Ru1‘ 87.06(11), Si1‘–C21‘–Ru2‘ 86.15(11), Ru2‘–C21‘–Ru1‘ 84.04(10), Ru2‘–N‘–Ru1‘ 77.74(7).

Two different polymorphs of compound **4** were obtained. A triclinic structure measured at 130 K and a monoclinic one measured at 100 K (see Figures S2 and S3 for packing diagrams). Both structures show a very distinct C–H…π contact between one of the hydrogen atoms at the NHC backbone and the Cp* ligand. The triclinic polymorph shows an additional contact between the Ruthenium atom and the *para*-hydrogen atom of a Dipp substituent whereas the corresponding distance in the monoclinic polymorph is significantly larger (see table S2 for metrical parameters).

Table S2. Metrical parameters of the two polymorphs of complex **4**.

polymorph	C19–H19	H19···Ru1	C19···Ru1	C19–H19···Ru1
triclinic	0.95 Å	3.1215(4) Å	4.0475(19) Å	165.30(15)°
monoclinic	0.95 Å	3.3075(3) Å	4.122(2) Å	145.03(15)°
	C–H	H···Centroid	C···Centroid	C–H···Centroid
triclinic	0.95 Å	2.5458(10) Å	3.485(3) Å	169.72(14)°
monoclinic	0.95 Å	2.6206(9) Å	3.530(2) Å	160.43(15)°

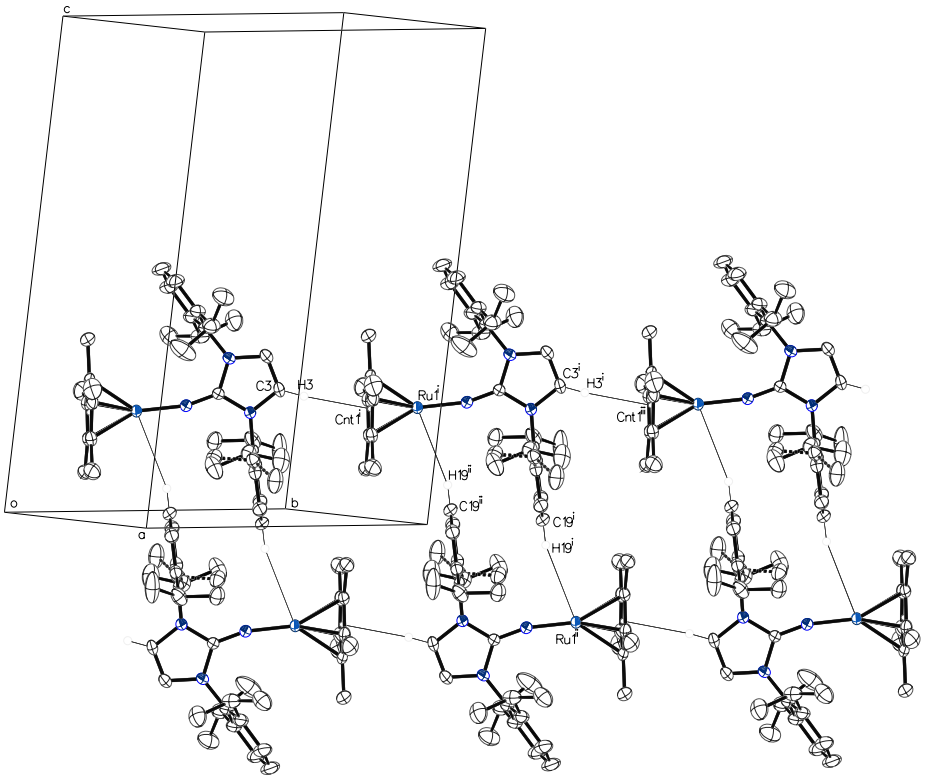

Figure S2. Packing diagram of the triclinic polymorph of **4** with thermal displacement parameters drawn at 50% probability. Hydrogen atoms except of H3 and H19 are omitted. The following symmetry operation have been applied: i) x, 1+y, z (translation), ii) 1-x, 2-y, 1-z (inversion) iii) x, 2+y, z (translation).

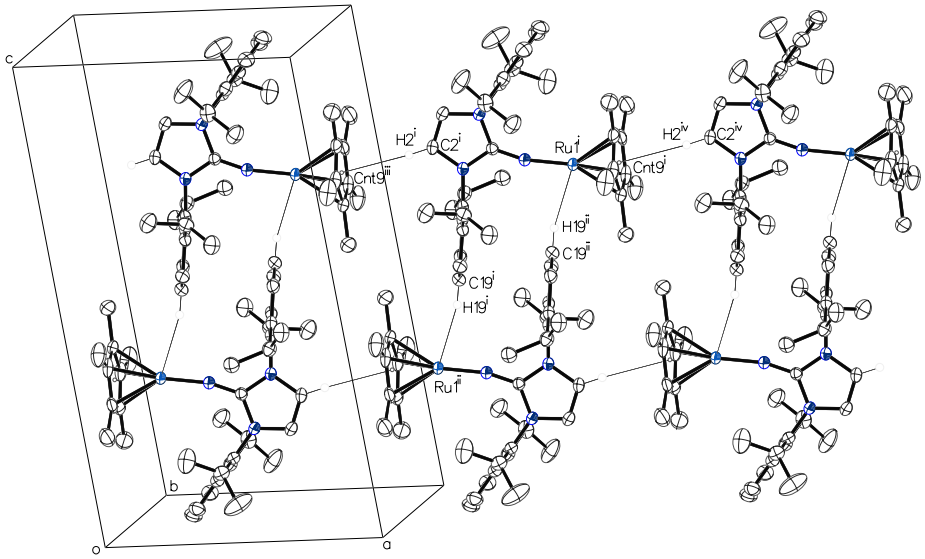

Figure S3. Packing diagram of the triclinic polymorph of **4** with thermal displacement parameters drawn at 50% probability. Hydrogen atoms except of H3 and H19 are omitted. The following symmetry operation have been applied: i) 2-x, 1-y, 1-z (inversion), ii) 1+x, y, z (translaion) iii) 1-x, 1-y, 1-z (inversion), iv) 3-x, 1-y, 1-z (inversion).

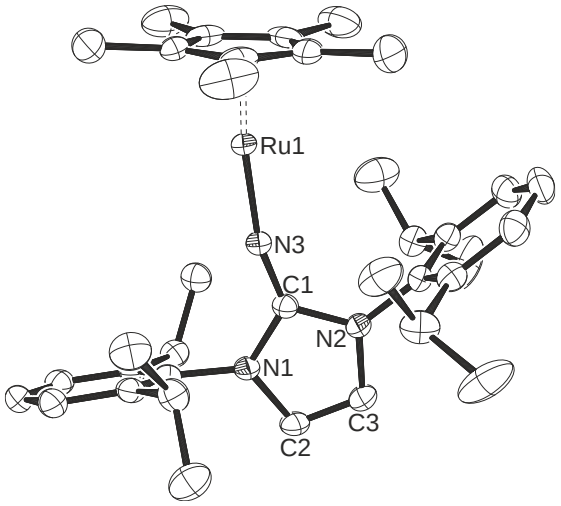

Figure S4. Molecular structure of compound **4** (monoclinic polymorph) with thermal displacement parameters drawn at 50% probability. Hydrogen atoms are omitted for clarity. Selected bond lengths [Å] and angles [°]: Ru–N3 1.8597(18), Ru–Cp*$_{centroid}$ 1.7609(10), N3–C1 1.291(3), N1–C1 1.381(3), N2–C1 1.384(3), Cp*$_{centroid}$–Ru–N3 172.61(7), Ru–N3–C1 166.18(16), N3–C1–N1 127.70(19), N3–C1–N2 128.00(18), N2–C1–N1 104.30(18).

S2 NMR spectra of new compounds

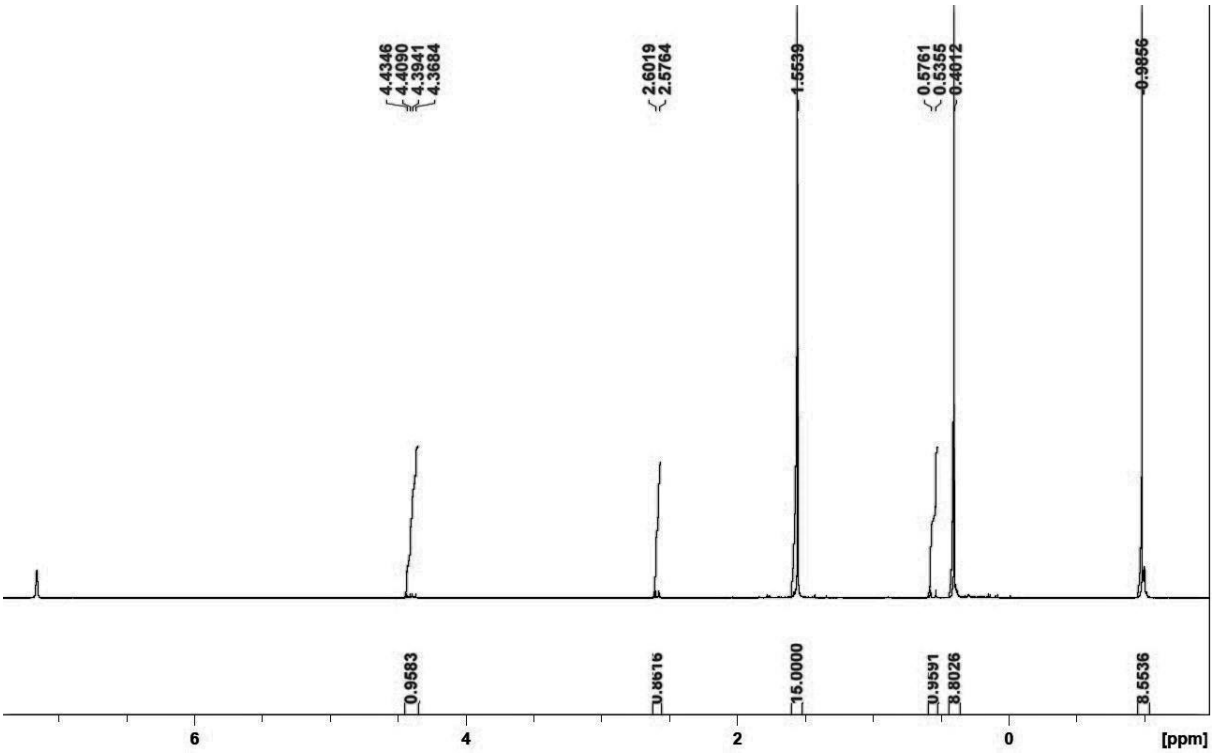

Figure S5. ^{1}H NMR spectra of **1** in C_6D_6.

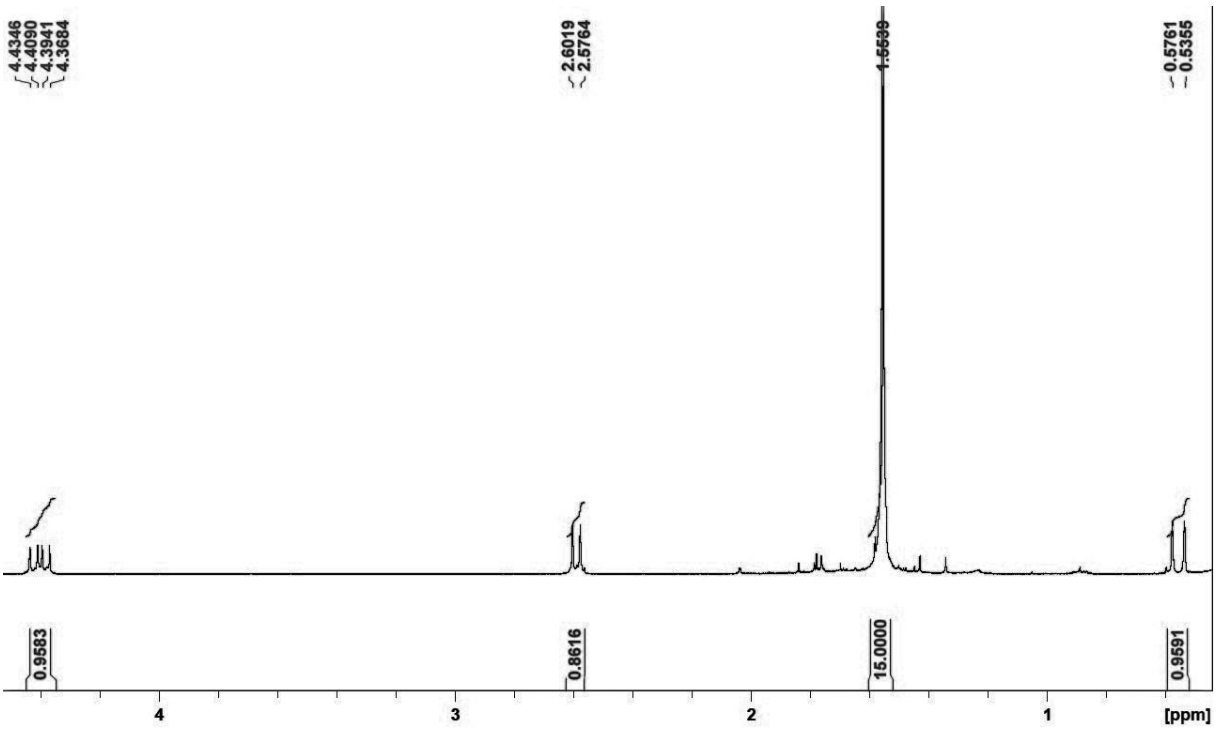

Figure S6. ^{1}H NMR spectra of **1** in C_6D_6 (expanded).

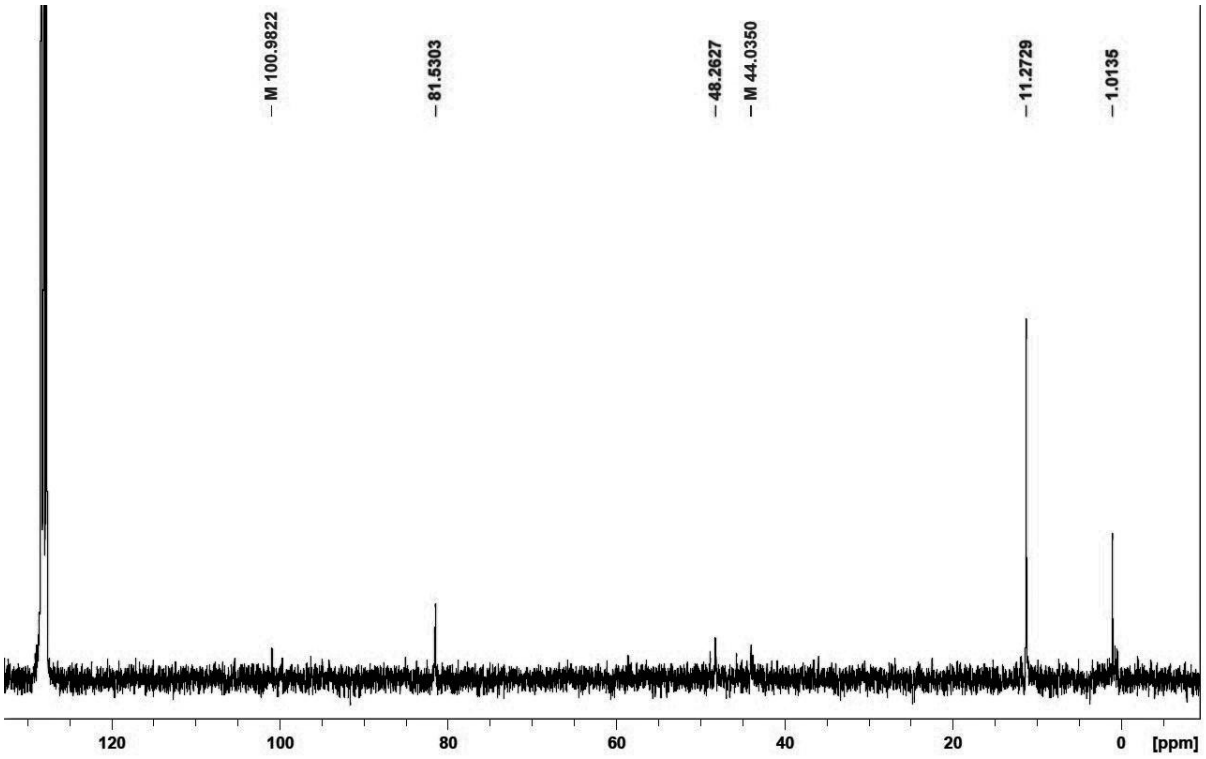

Figure S7. $^{13}C\{^{1}H\}$ NMR spectra of **1** in C_6D_6.

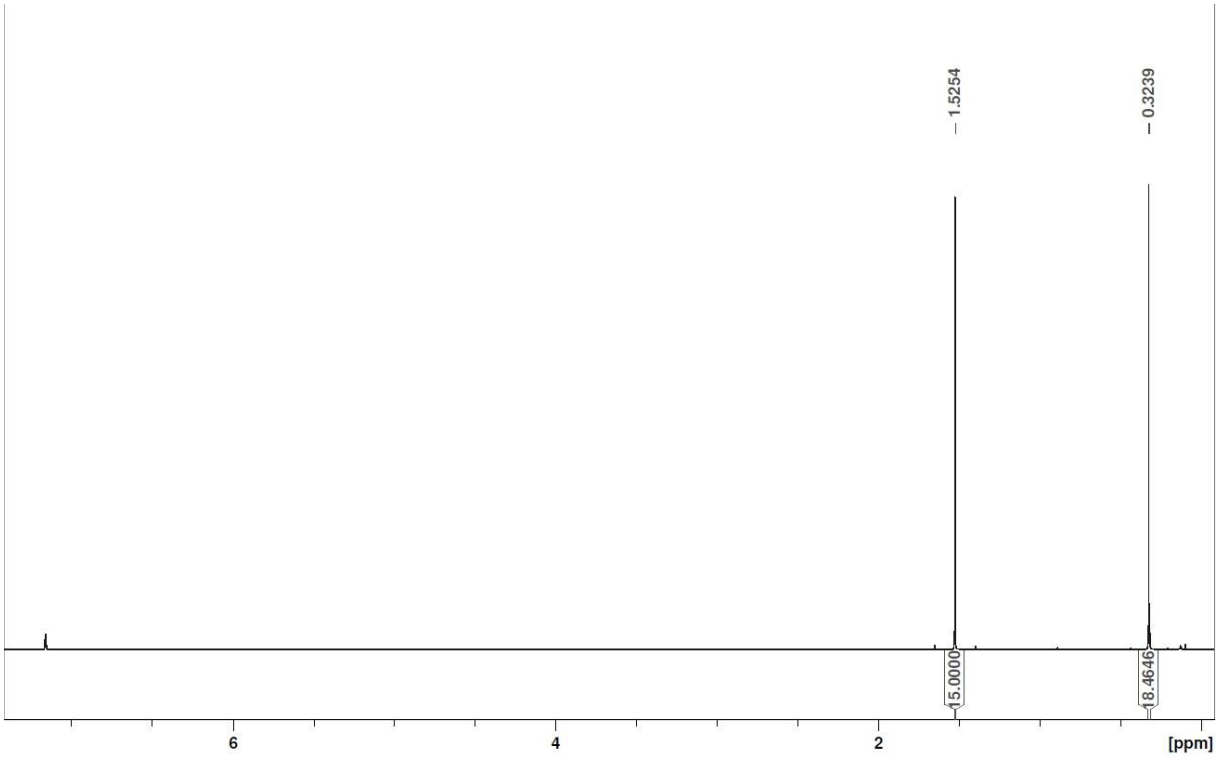

Figure S8. ^{1}H NMR spectra of **2** in C_6D_6.

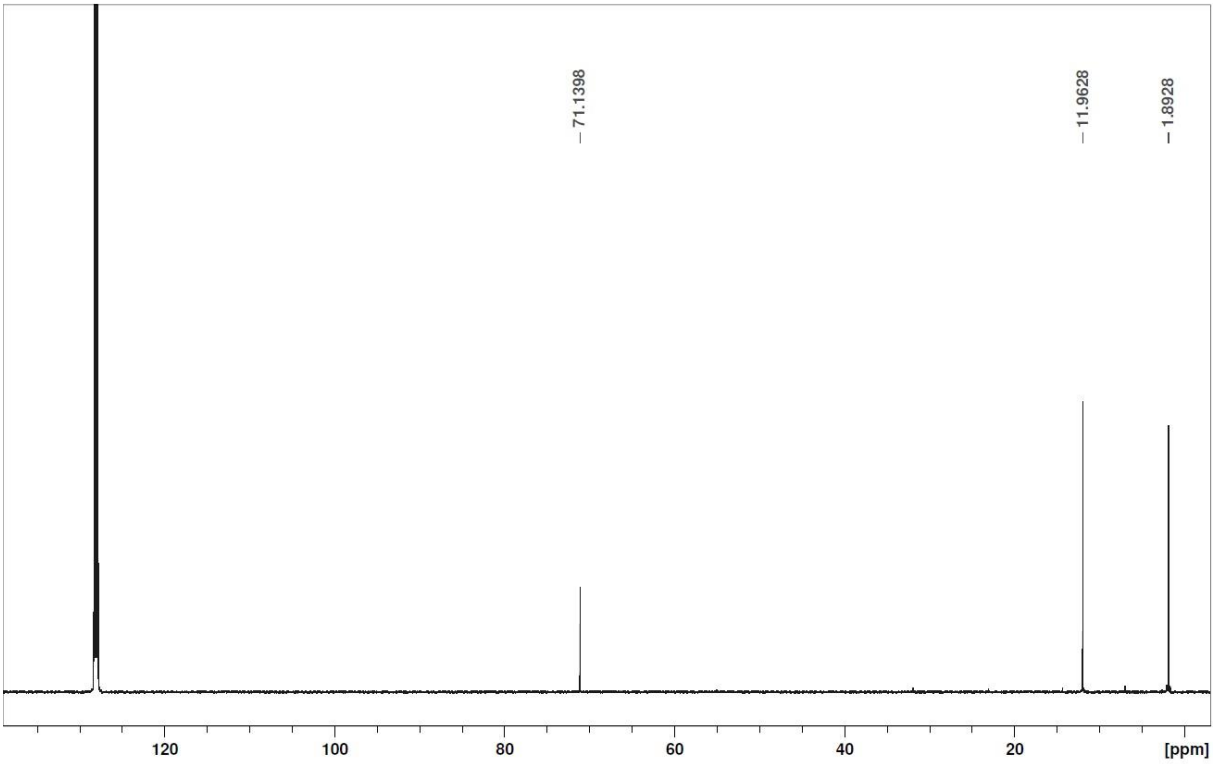

Figure S9. $^{13}C\{^{1}H\}$ NMR spectra of **2** in C_6D_6.

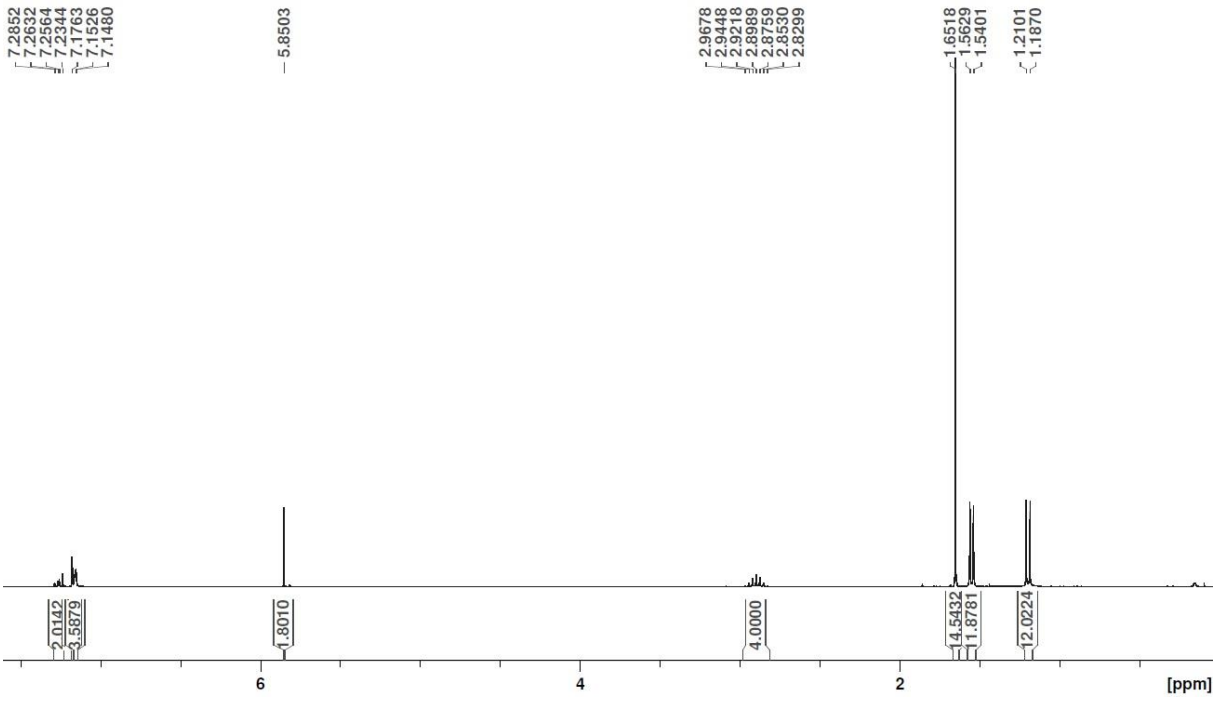

Figure S10. ^{1}H NMR spectra of **4** in C_6D_6 by Method 1.

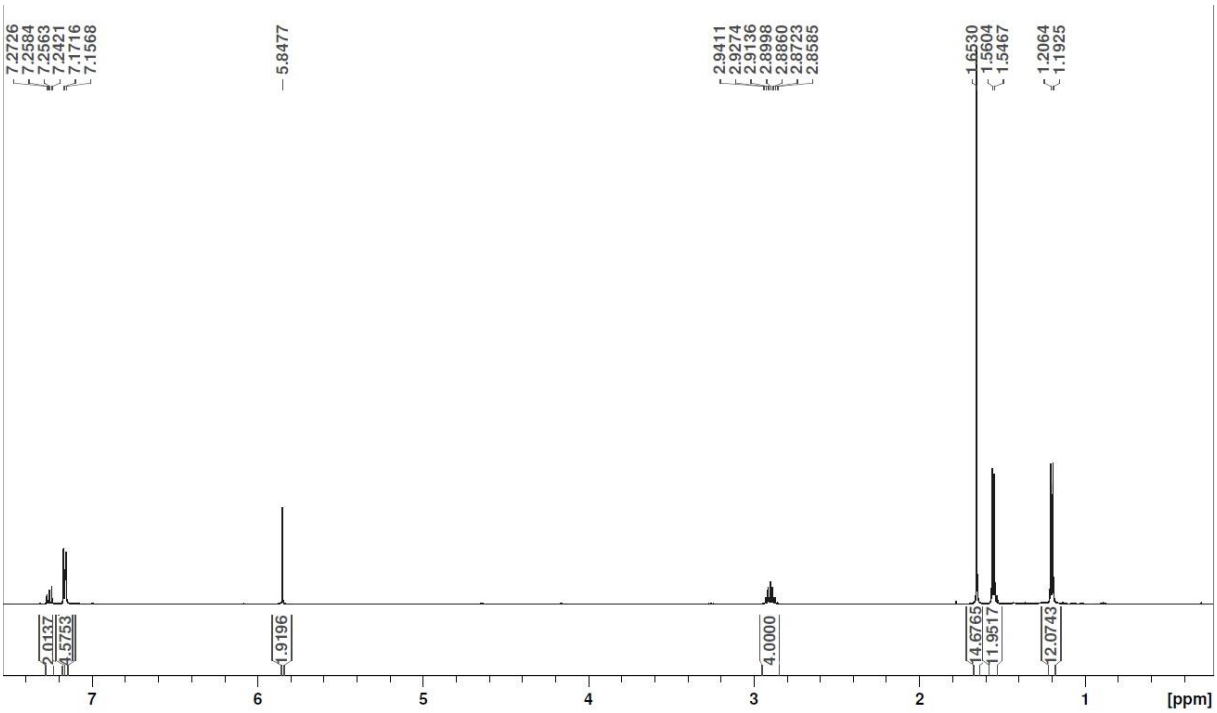

Figure S11. ^{1}H NMR spectra of **4** in C_6D_6 by Method 2.

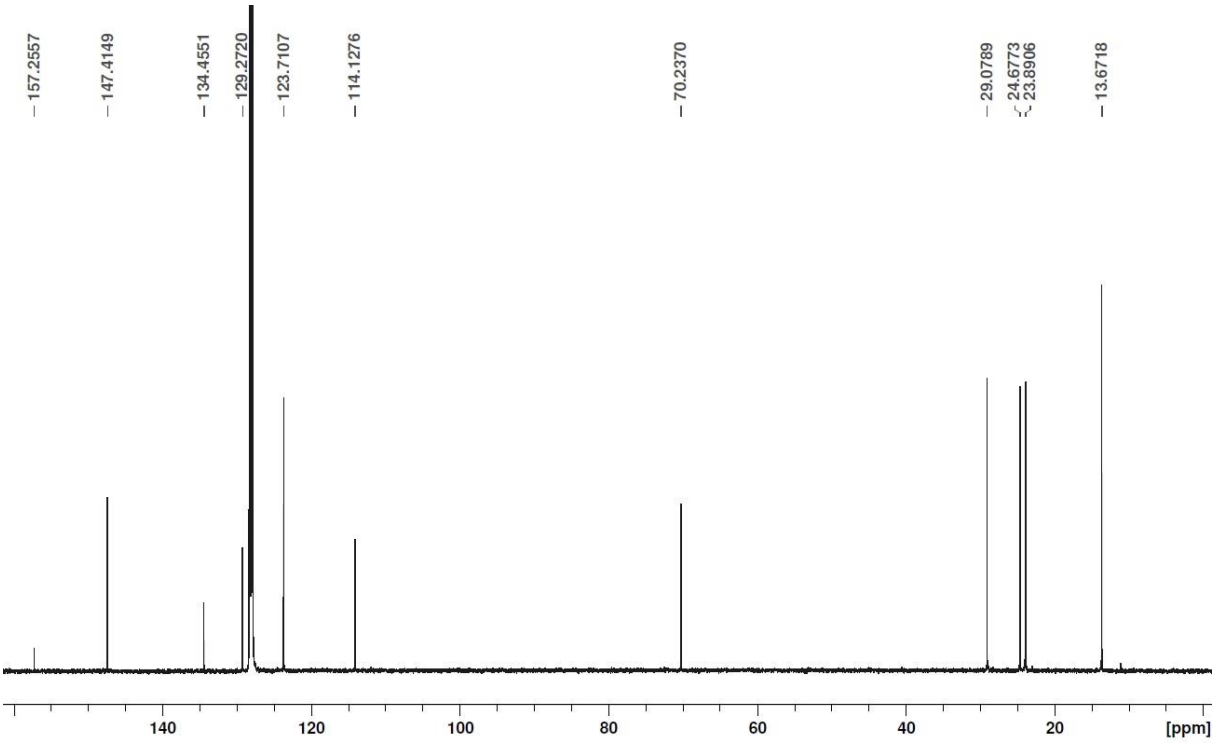

Figure S12. $^{13}C\{^{1}H\}$ NMR spectra of **4** in C_6D_6.

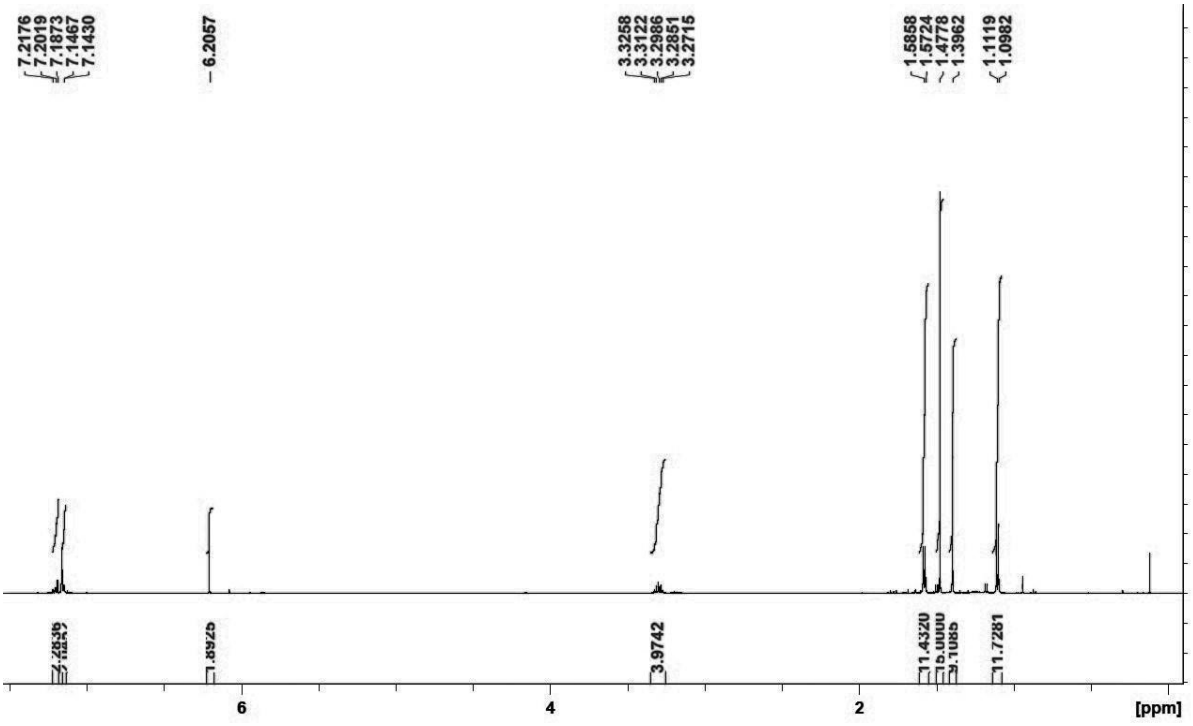

Figure S13. ^{1}H NMR spectra of **5** in C_6D_6.

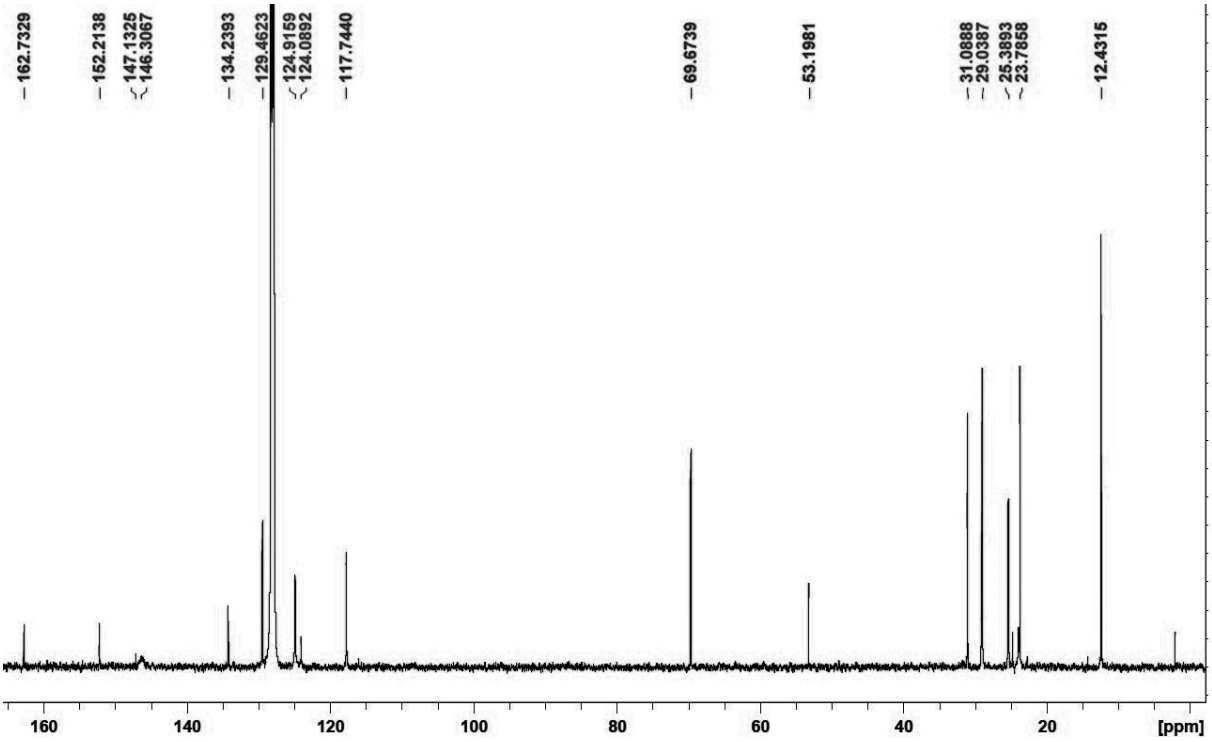

Figure S14. $^{13}C\{^{1}H\}$ NMR spectra of **5** in C_6D_6.

S3 NMR studies of complex 2

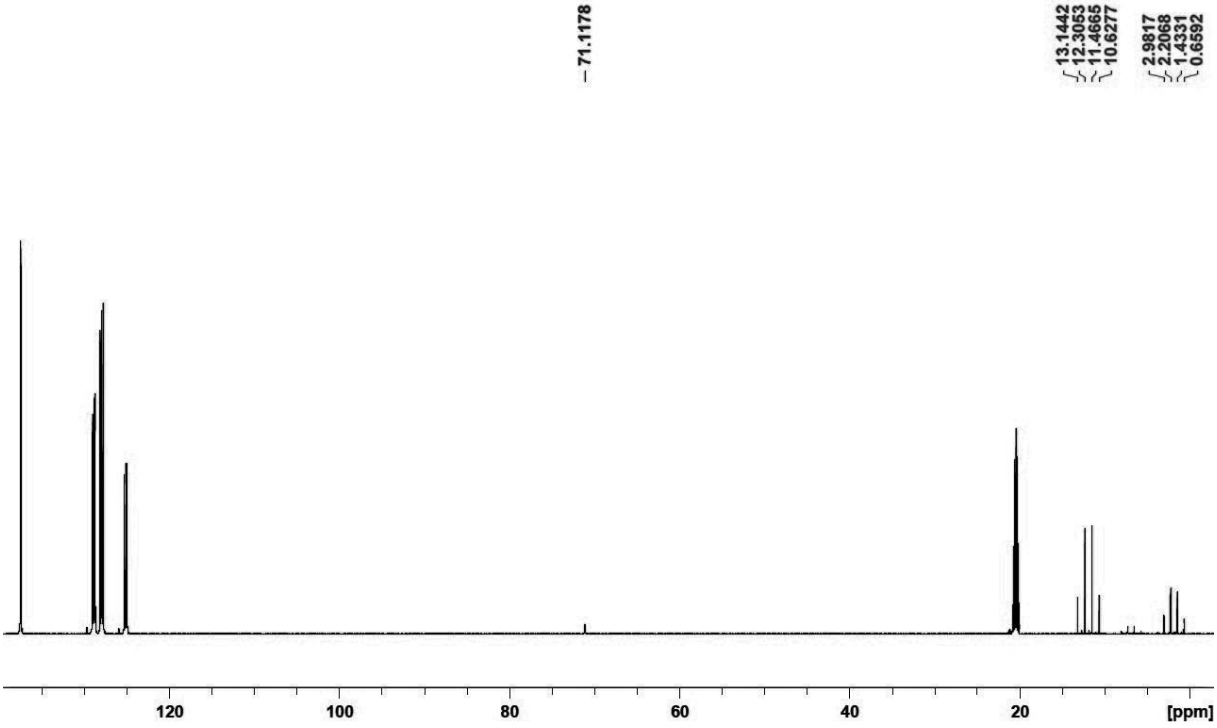

Figure S15. ^{13}C gated decoupled NMR spectra of **2** at room temperature in toluene-d_8.

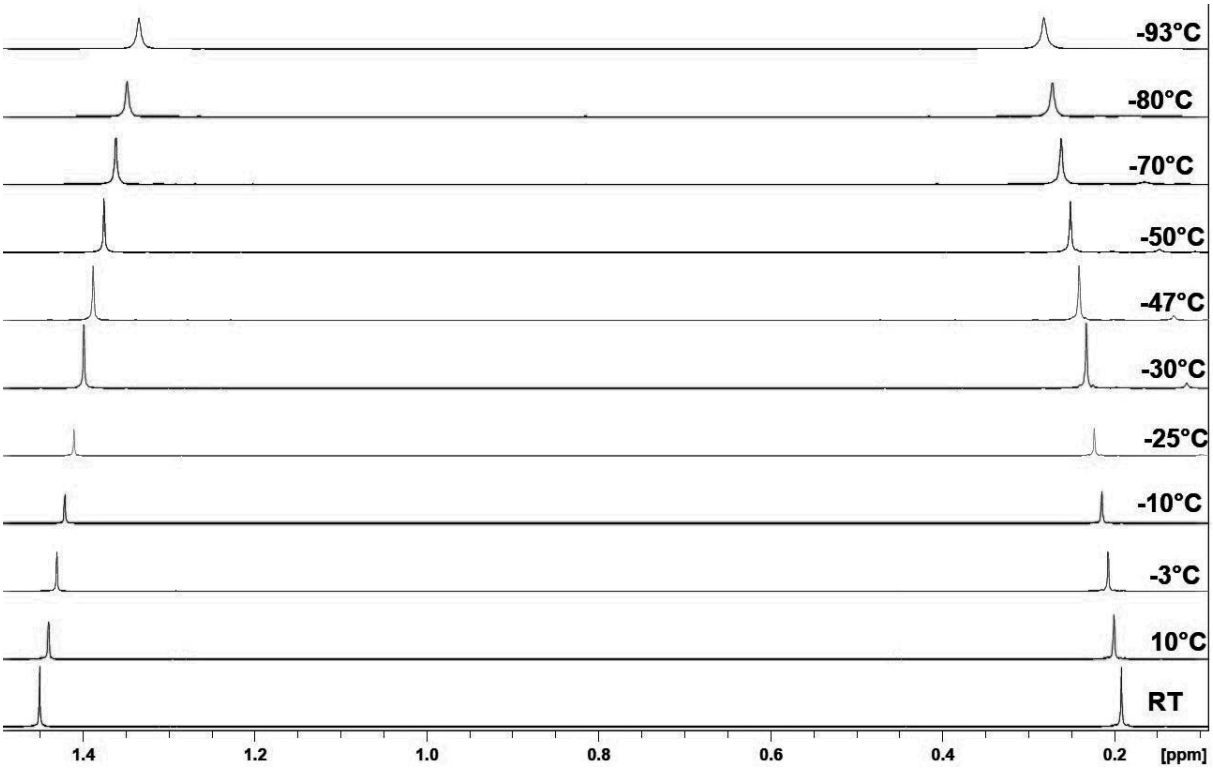

Figure S16. ^{1}H Variable temperature NMRs of **2** in toluene-d_8.

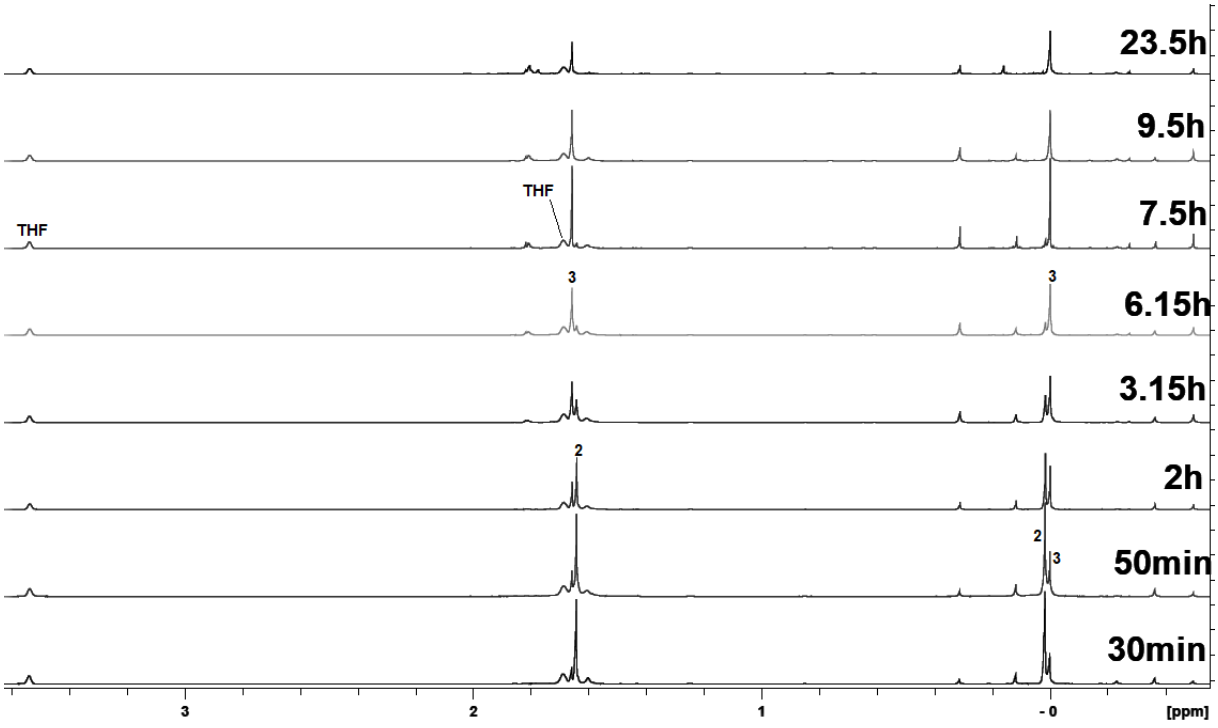

Figure S17. ^{1}H NMR study of complex **2** in THF-d_8.

S4 Computational Details

All computations were performed using the density functional method M06-L as implemented in the Gaussian09 program.[5] For all elements (C, H, N, Si and Ru) the newer redefinitions of Ahlrichs triple-ζ basis sets def2-TZVP (*"Karlsruhe basis sets"*) were applied.[6] The QTAIM analysis of the wave function was performed using the freely available program package *MultiWFN 3.6*[7] and the binding analysis of complex **4** was done with the free program *GaussSum 3.0*.[8] Calculations have been carried out in the gas phase.

Table S3: Energies of all Optimized Structures

compound	E_{0K} [a] [Ha]	E_{298K} [b] [Ha]	H_{298K} [b] [Ha]	G_{298K} [b] [Ha]
syn,anti-[(η^5-C_5Me_5)Ru{η^3-$C_3H_3(SiMe_3)_2$}] (**1**)	-1419.482563	-1419.450596	-1419.449652	-1419.542043
syn,syn-[(η^5-C_5Me_5)Ru{η^3-$C_3H_3(SiMe_3)_2$}]	-1419.475420	-1419.442446	-1419.441502	-1419.537897
[(η^5-C_5Me_5)Ru{$N(SiMe_3)_2$}] (**2**)	-1358.194704	-1358.164376	-1358.163432	-1358.252948
[(η^5-C_5Me_5)Ru(NIm^{Dipp})] (**4**)	-1699.516894	-1699.472370	-1699.471425	-1699.592693

[a] DFT energy incl. ZPE. [b] standard conditions T = 298.15 K and p = 1 atm.

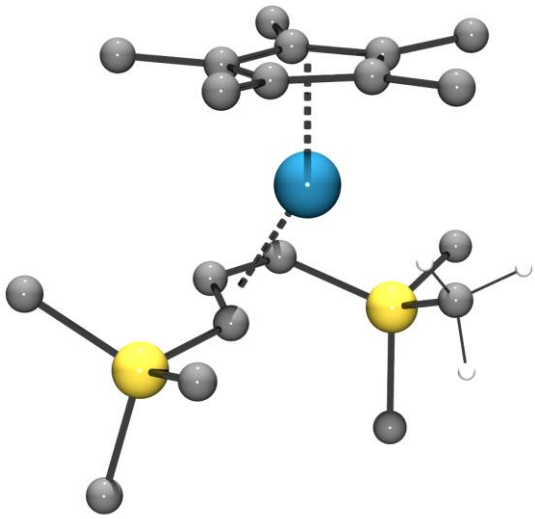

Figure S18. Ball-and-stick model of **1** (*syn,anti* orientation). (Grey: C, Blue: Ru, Yellow: Si, White: H; Hydrogen atoms omitted for clarity, except at C50).

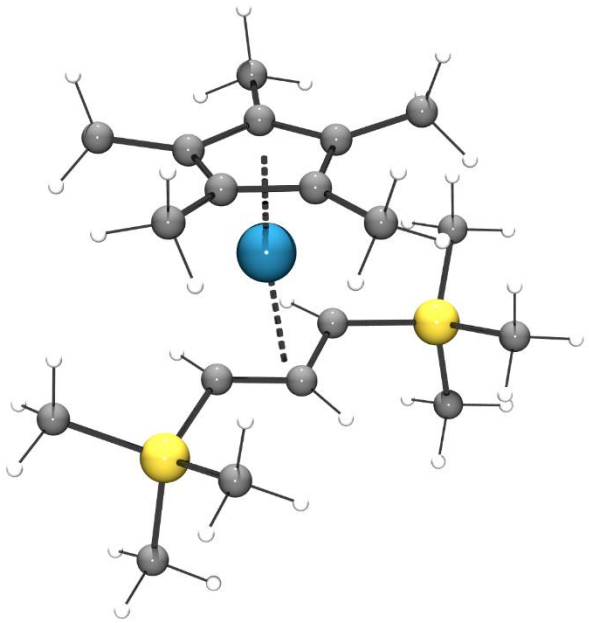

Figure S19. Ball-and-stick model of **1** (*syn*,*syn* orientation). (Grey: C, Blue: Ru, Yellow: Si, White: H).

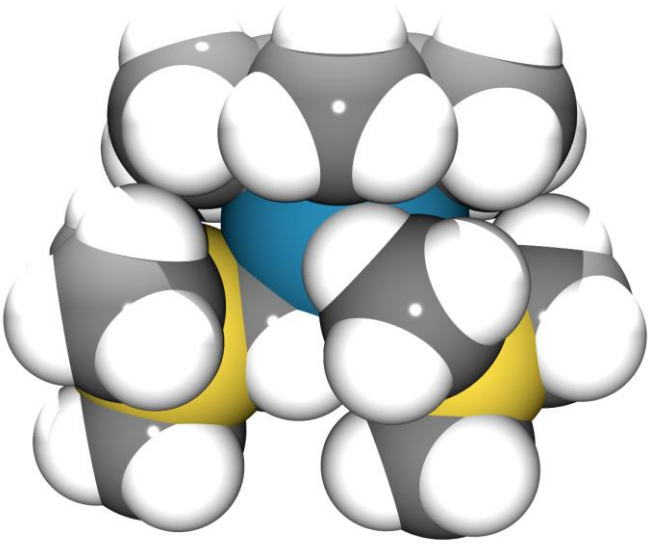

Figure S20. Space-filling model of **1** (*syn*,*anti* orientation). (Grey: C, Blue: Ru, Yellow: Si, White: H).

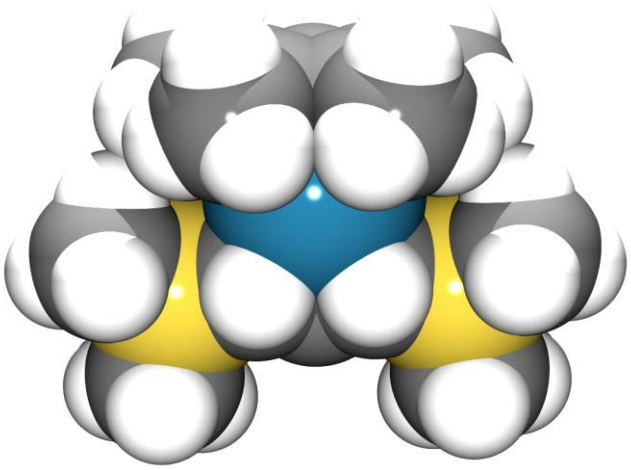

Figure S21. Space-filling model of **1** (*syn*,*syn* orientation). (Grey: C, Blue: Ru, Yellow: Si, White: H).

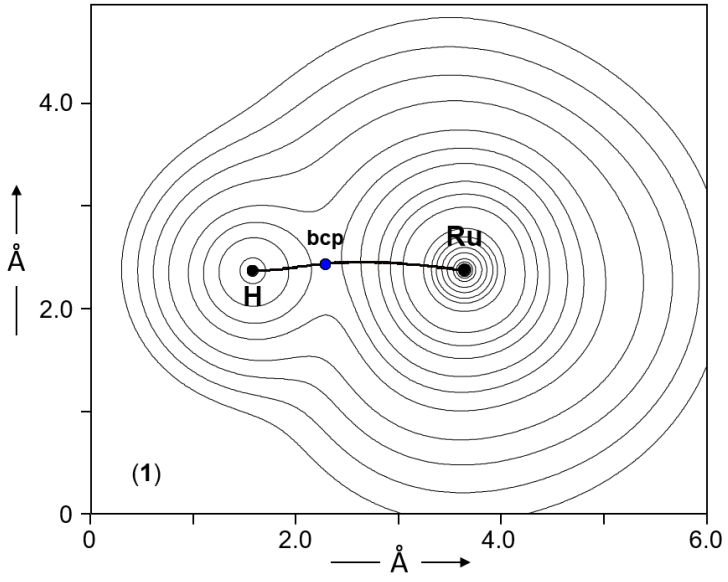

Figure S22. Counterplot of the electron density $\rho(\boldsymbol{r})$ of complex **1**. The solid blue point marks (3,-1) bond critical points (bcp). Gaussian DFT calculation: M06-L/def2-TZVP

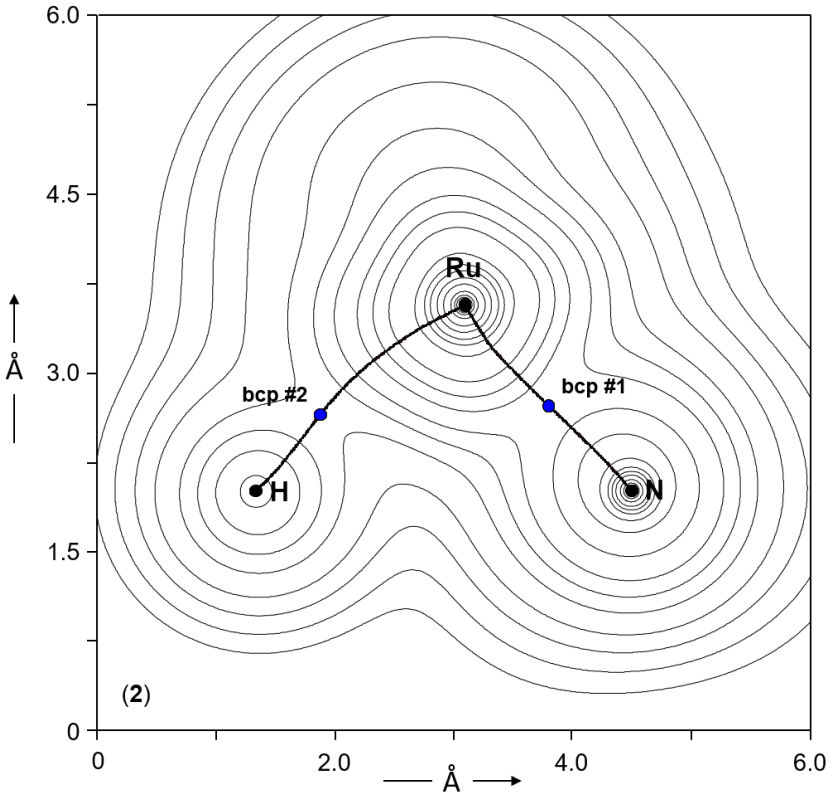

Figure S23. Counterplot of the electron density $\rho(\boldsymbol{r})$ of complex **2**. The solid blue point marks (3,-1) bond critical points (bcp). Gaussian DFT calculation: M06-L/def2-TZVP

S5 References

[1] Rigaku Oxford Diffraction, *CrysAlisPRO Software System*, versions 1.171.37.43 (**2015**) and 1.171.38.43c (**2015**), Rigaku Corporation, Oxford, UK.

[2] G. M. Sheldrick, *Acta Cryst.*, 2015, **A71**, 3-8

[3] G. M. Sheldrick, *Acta Cryst*., 2008, **A64**, 112-122

[4] G. M. Sheldrick, *Acta Cryst.*, 2015, **C71**, 3-8

[5] Gaussian 09, Revision D.01, M. J. Frisch, G. W. Trucks, H. B. Schlegel, G. E. Scuseria, M. A. Robb, J. R. Cheeseman, G. Scalmani, V. Barone, G. A. Petersson, H. Nakatsuji, X. Li, M. Caricato, A. Marenich, J. Bloino, B. G. Janesko, R. Gomperts, B. Mennucci, H. P. Hratchian, J. V. Ortiz, A. F. Izmaylov, J. L. Sonnenberg, D. Williams-Young, F. Ding, F. Lipparini, F. Egidi, J. Goings, B. Peng, A. Petrone, T. Henderson, D. Ranasinghe, V. G. Zakrzewski, J. Gao, N. Rega, G. Zheng, W. Liang, M. Hada, M. Ehara, K. Toyota, R. Fukuda, J. Hasegawa, M. Ishida, T. Nakajima, Y. Honda, O. Kitao, H. Nakai, T. Vreven, K. Throssell, J. A. Montgomery, Jr., J. E. Peralta, F. Ogliaro, M. Bearpark, J. J. Heyd, E. Brothers, K. N. Kudin, V. N. Staroverov, T. Keith, R. Kobayashi, J. Normand, K. Raghavachari, A. Rendell, J. C. Burant, S. S. Iyengar, J. Tomasi, M. Cossi, J. M. Millam, M. Klene, C. Adamo, R. Cammi, J. W. Ochterski, R. L. Martin, K. Morokuma, O. Farkas, J. B. Foresman, and D. J. Fox, Gaussian, Inc., Wallingford CT, **2016**.

[6] a) F. Weigend, R. Ahlrichs, *Phys. Chem. Chem. Phys.*, 2005, **7**, 3297–3305. b) F. Weigend, *Phys. Chem. Chem. Phys.*, 2006, **8**, 1057–1065.

[7] a) T. Lu, F. Chen, *J. Comput. Chem.* 2012, 33, 580–592. b) The program **MultiWFN 3.6** is available at: http://sobereva.com/multiwfn/.

[8] (a) N. M. O'Boyle, A. L. Tenderholt, K. M. Langner, *J. Comput. Chem.*, 2007, **29**, 839–845. b) The program **GaussSum 3.0** is available at http://gausssum.sourceforge.net/.